Hao Liang, Ke Zhang, Zhongyun Li, Jianli Fu, Zhangxin Yu, Jianguo Xiong, Xiaoyang Li, Zhanwu Ma, Ping Huang, Zhigang Li, Yipeng Zhang, Gege Hui, Qinying Tian, Weitao Wang, Wenjun Zheng, and Peizhen Zhang, 2022, How headward erosion breaches upstream paleolakes: Insights from dated longitudinal fluvial terrace correlations within the Sanmen Gorge, Yellow River: GSA Bulletin, https://doi.org/10.1130/B36537.1.

Supplemental Material

Text. Lithostratigraphy; Field Sampling, methods, and pretreatments; Terrace description in basin area.

Table S1. Established ages of the Chinese loess-paleosol sequence

Table S2. Geographic information for terrace strath locations in the Sanmen Gorge

Table S3. Geographic information for erosional landform locations in the Sanmen Gorge

Figure S1. De distributions for OSL samples. All radial plots are centered on the CAM weighted mean De value, and points that lie within the shaded region are within 2 standard deviations of the CAM weighted mean.

Figure S2. Luminescence signals and decay curves of OSL samples, from top to bottom are ST-1, ST-2, ST-3, ST-4, ST-5, ST-6, ST-7, respectively.

Figure S3. Photos of fluvial landforms and deposits. (a). Gravels capped by paleosol S_2 in T_2 at Site 4; (b). Pebbly sand capped by paleosol S_5 in T_3 at Site 4; (c). Details of the pebbly sand in T_3 at Site 4; (d). Gravels capped by paleosol S_{23} in T_5 at Site 6. (e). Erosional platform intervening the Site 1 and Site 2, note that the higher one locates the Terrace 1 correlation; (f). The hanging valley outlet and erosional caves intervening the Site 1 and Site I; note that the hanging valley outlet locates the Terrace 2 correlation.

I. LITHOSTRATIGRAPHY

A. LITHOFACIES DESCRIPTIONS AND INTERPRETATIONS

Table.S1 Established ages of the Chinese loess-paleosol sequence

Unit of loess stratigraphy	Marine oxygen isotope stage	Age (ka)
S_0	MIS1	0–11
S_1	MIS5	73–128
S_2	MIS7	190–245
S_3	MIS9	307–336
S_4	MIS11	360–412
S_5	MIS13–15	479–621
S_8	MIS21	819–865
S_{10}	MIS29	1018–1049
S_{14}	MIS37	1220–1240
S_{23}	MIS55–57	1588–1648

Correlation of the paleosol units with marine oxygen isotope stages is according to Ding et al. (2002).

II. FIELD SAMPLING, METHODS AND PRETREATMENTS

A. OPTICALLY STIMULATED LUMINESCENCE (OSL) DATING

We excavated ~20cm inside the original loess succession after removal of the capping material and soil to reduce potential error. Samples were retrieved by hammering light-tight steel tubes (diameter 5 cm, length 15 cm) horizontally into the exposure without exposing to light and subsequently wrapped in foil paper. Samples for environmental dose rate measurement were collected from the material surround the tubes.

Sample preparation were carried out under red-light condition. Approximate 4 cm of material at each portion of sample tubes was removed and reserved for environment does rate measurement. The relic unexposed part in tubes was used to determine equivalent does (De). All samples were first added 10% HCl to dissolve carbonates, then added 30% H_2O_2 to dissolve organic matter. After dissolving, the 4–11μm grain size fraction was extracted by wet sieving. Heavy liquids with density of 2.62 g/cm^3 and 2.58 g/ cm^3 were used to separate the quartz and K-feldspar fractions of each sample, respectively. The quartz samples were treated with fluosilicate (H_2SiF_6) for one week and with 10% HCl to remove fluorides. The K-feldspar samples were excluded by acid etch to avoid preferentially attack of cleavage planes rather than removing a uniform shell from grains. The purified quartz and K-feldspar grains were mounted on the central part of stainless-steel discs (ca. 0.97 cm diameter) by silicone oil. All discs were measured by automated Risø TL/OSL-DA-20 reader with $^{90}Sr/^{90}Y$ sources. The OSL signal was obtained by passage through a Hoya U-340 filter for quartz grains and a photomultiplier tube with BG-39 and coring-759 filters for feldspar grains. Chemical analyses of OSL samples were carried out using the Agilent 7700 inductively coupled plasma-mass spectrometry (ICP-MS) and inductively coupled plasma-atomic emission spectrometry (ICP-AES) to determine U and Th concentration and K content, respectively. The concentrations were converted to environmental dose rates (Gy/ka) according to method of Adamiec and Aitken (1998). Contribution of cosmic ray to the does rate was based on techniques of Prescott and Hutton (1994).

Measurement on quartz were using single aliquot regeneration (SAR) described by Murray and Wintle (2000), a post-IR IRSL procedure based on Colarossi et al. (2015) was used for K-feldspar. Preheat temperatures ranged from 180 to 300 °C at 20 °C intervals for 10s with a heating rate of 5 °C/s, and fixed the cut-heat temperature at 200 °C for both quartz and feldspar De value measurements. Feldspar post-IR IRSL De value was determined by integrating the initial 4 of the decay curves after subtraction of a late background, taken from the last 20 s of the decay curve. Acceptance criteria for the K-feldspar data required individual aliquots to have recycling ratios within 10% of unity, and recuperation less than 5% of the natural signal.

The total dose (De) for each sample was modeled using the central age model (CAM) of Galbraith et al. (1999) that models the central tendency taking into account the over-dispersion of the error associated with each aliquot measurement. Radial plots (Fig. S1) were used to examine the distribution of De values. Over-dispersion values are low (<10%) and the De distributions are nearly symmetrical, suggesting that most grains were sufficiently bleached prior to burial.

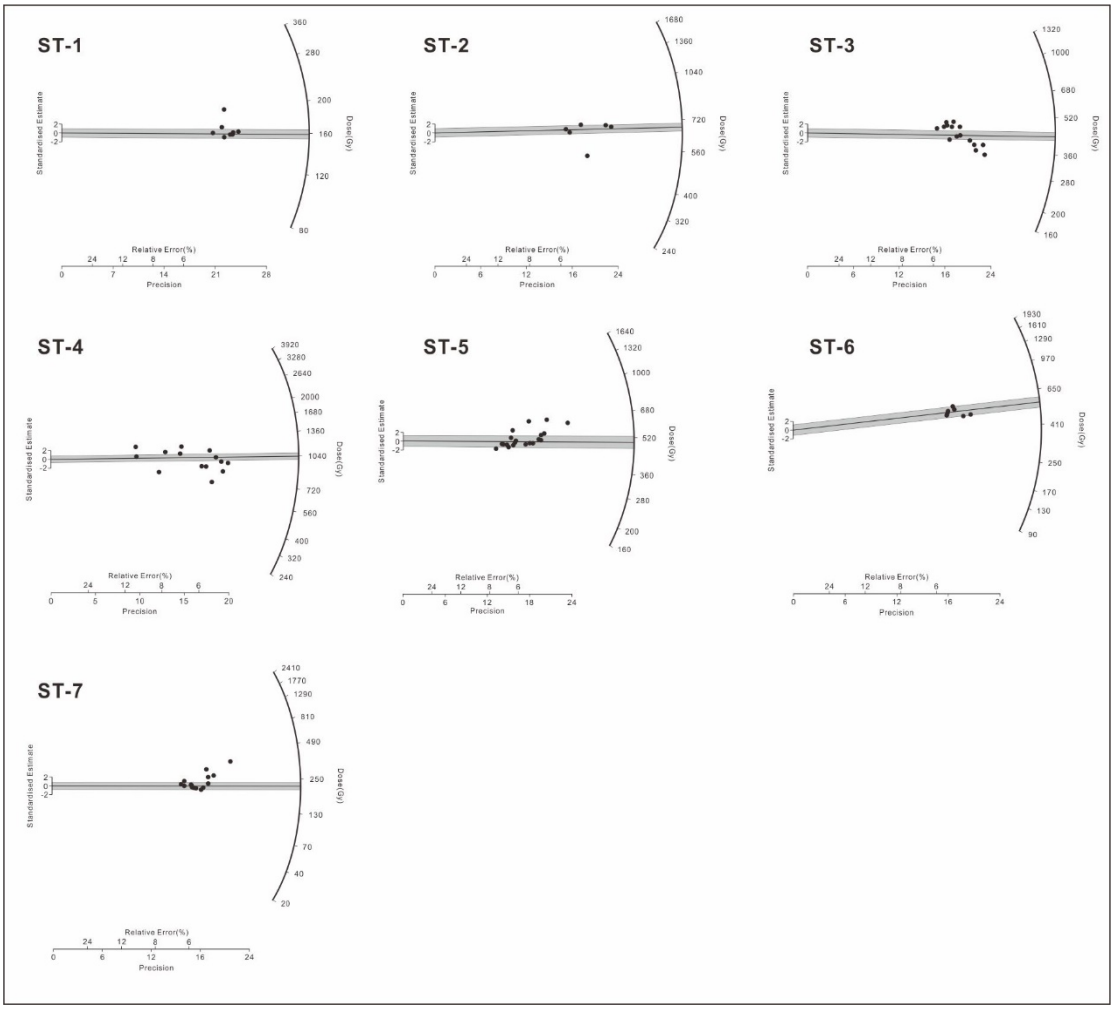

Figure S1. De distributions for OSL samples. All radial plots are centered on the CAM weighted mean De value, and points that lie within the shaded region are within 2 standard deviations of the CAM weighted mean.

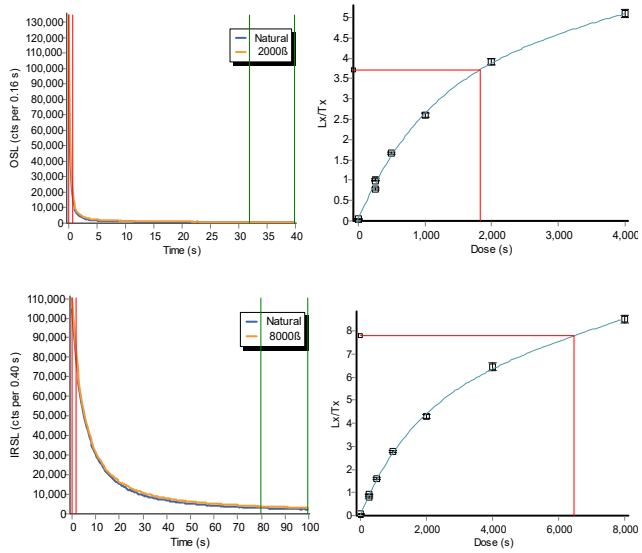

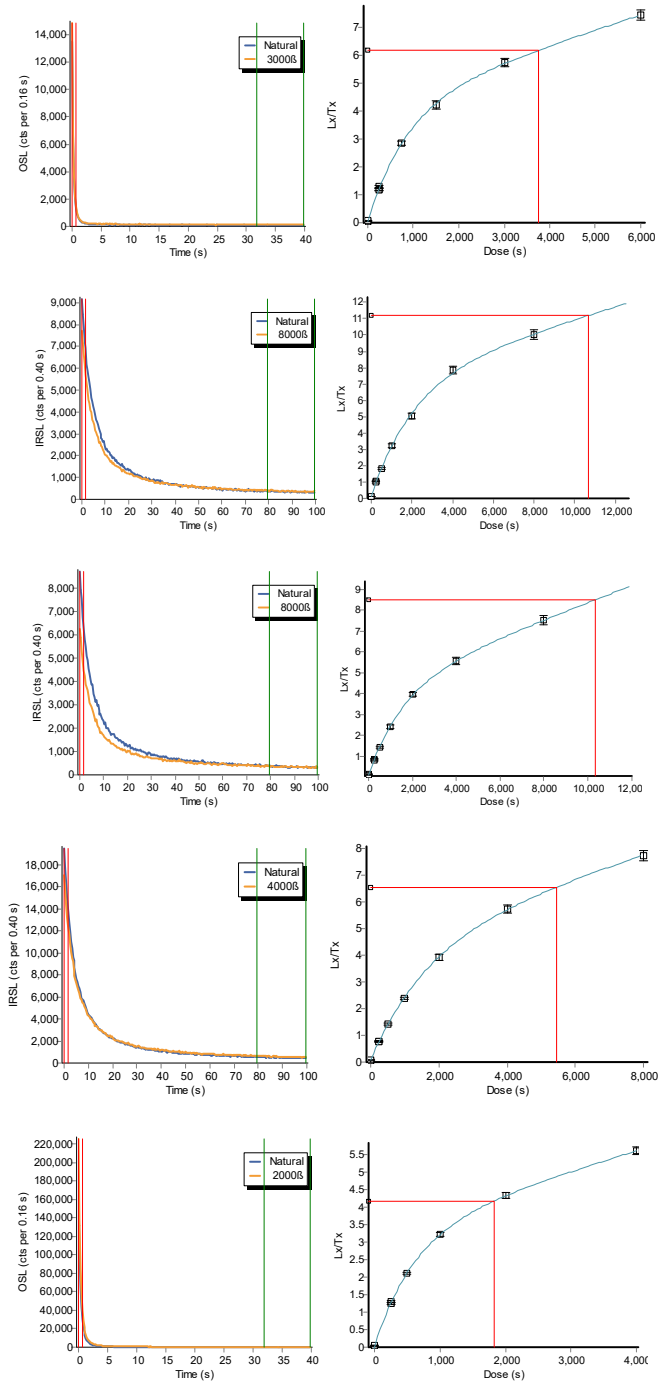

Figure S2. Luminescence signals and decay curves of OSL samples, from top to bottom are ST-1, ST-2, ST-3, ST-4, ST-5, ST-6, ST-7, respectively.

For magnetic susceptibility measurements, samples were collected at 0.1 m intervals from the loess succession. Samples were packed in 8cm^3 plastic boxes following air-dried and disaggregated. Mass magnetic susceptibility were measured using a Bartington MS2B magnetic susceptibility meter.

III. TERRACE DESCRIPTION IN BASIN AREA

A. ADDITIONAL IMFORMATION OF TERRCES IN THE SANMEN GORGE

Table.S2 Geographic information for terrace strath locations in the Sanmen Gorge

ID	Terrace Site	Terrace name	Strath elevation (m a.s.l)[a]	Latitude	Longitude	Reference
	Site 1			34°49′1.1”	111°23′11.5”	
1		T1	272			This study
2		T2	305			This study
3		T3	330			This study
4		T4	356			This study
	Site 2			34°50′3.00”	111°28′59.6”	
5		T1	256			This study
6		T2	280			This study
7		T3	296			This study
8		T4	343			This study
	Site 3			34°50′49.1”	111°33′43.4”	
9		T1	255			This study
10		T2	281			This study
11		T3	315			This study
12		T4	330			This study
	Site 4			34°53′17.9”	111°36′22.3”	
13		T1	280			This study
14		T2	304			Fu (2009)
15		T3	328			Fu (2009)
	Site 5			34°55′30.3”	111°37′11.9”	
16		T1	266			This study
17		T2	287			This study
18		T3	296			This study
19		T4	305			This study
	Site 6			35° 2′36.0”	111°47′40.4”	
20		T1	248			This study
21		T2	258			This study
22		T3	299			Fu (2009)
23		T4	356			This study
24		T5	406			Fu (2009)
	Site 7			35° 1′58.7”	112° 5′42.3”	
25		T1	235			Fu (2009)
26		T2	257			This study
27		T3	303			This study
28		T4	446			This study
	Site 8			34°54′53.2”	112°27′29.5”	
29		T1	145			Meng et al. (2015)
30		T2	235			Meng et al. (2015)
31		T3	265			Meng et al. (2015)
32		T4	281			This study
33		T5	300			This study

[a] m a.s.l-Meters above sea level.

Table S3. Geographic information for erosional landform locations in the Sanmen Gorge

ID	Terrace Site	Marks	elevation (m a.s.l)[a]	Latitude	Longitude
1	Site 1	Hanging valley outlet	338	34°49′1.1”	111°23′11.5”
2		Hanging valley outlet	336		
3	Site 2	Erosional platform	348	34°50′3.00”	111°28′59.6”
4		Erosional platform	349		
5	Site 4	Hanging valley outlet	300	34°53′17.9”	111°36′22.3”
6		Hanging valley outlet	302		

[a] m a.s.l-Meters above sea level.

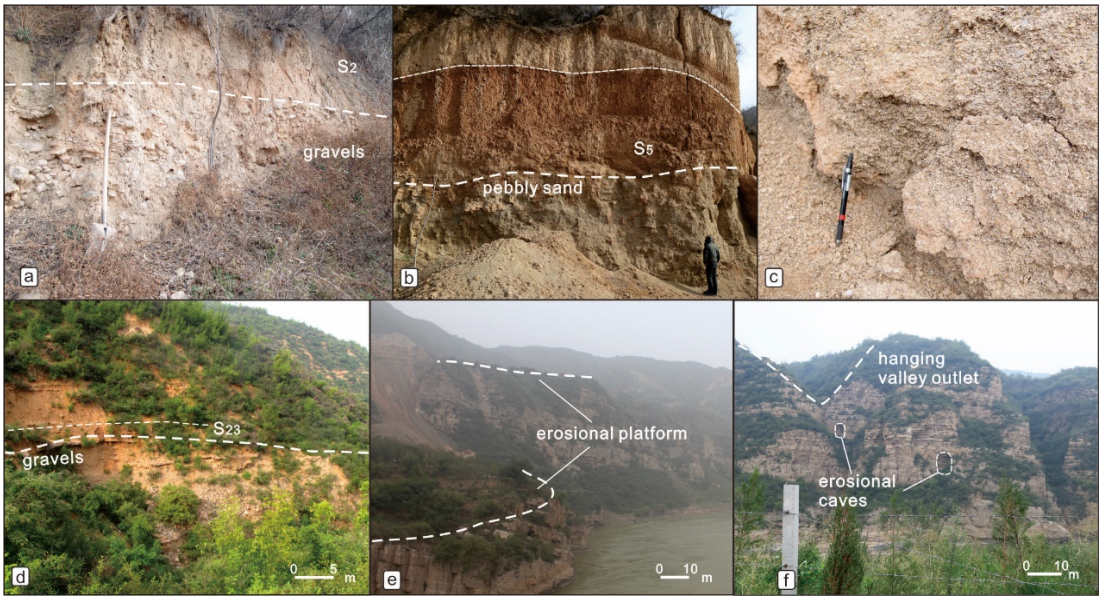

Fig.S3. Photos of fluvial landforms and deposits. (a). Gravels capped by paleosol S_2 in T_2 at Site 4; (b). Pebbly sand capped by paleosol S_5 in T_3 at Site 4; (c). Details of the pebbly sand in T_3 at Site 4; (d). Gravels capped by paleosol S_{23} in T_5 at Site 6. (e). Erosional platform intervening the Site 1 and Site 2, note that the higher one locates the Terrace 1 correlation; (f). The hanging valley outlet and erosional caves intervening the Site 1 and Site I; note that the hanging valley outlet locates the Terrace 2 correlation;

B. TERRACE DESCRIPTION IN BASIN AREA

Profile K

Three terraces developed on lacustrine deposits at the site of Profiles K. The T_1 terrace (397 m a.s.l.) manifests extensive tread without loess. The T_2 (410 m a.s.l.) terrace is characterized coarse sand enclosing pebbles with 5m-thick overlying loess. The T_3 (440 m a.s.l.) terrace consists of 20m-thick pebbly coarse sand and is covered by 15m-thick loess with S_2 paleosol at the base (Fu et al., 2013).

Profile N

Two terraces developed on lacustrine deposits at the site of Profiles N. The T_1 terrace (366 m a.s.l.) is covered by 14m-thick loess. The T_2 (382 m a.s.l.) terrace is characterized 3m-thick pebbly coarse sand and is covered by with 23m-thick overlying loess with S_2 paleosol at the base (Li et al., 2020).

Profile I

Two terraces developed on lacustrine deposits at the site of Profiles I. The T_1 terrace (320 m a.s.l.) is covered by 10m-thick loess. The T_2 (352 m a.s.l.) terrace is characterized 12m-thick pebbly coarse sand and is covered by with 20m-thick overlying loess with S_2 paleosol at the base (Wang et al., 2013).

REFERENCES CITED

Colarossi, D., Duller, G.A.T., Roberts, H.M., Tooth, S., and Lyons, R., 2015, Comparison of paired quartz OSL and feldspar post-IR IRSL dose distributions in poorly bleached fluvial sediments from South Africa: Quaternary Geochronology, v. 30, p. 233–238, https://doi.org/10.1016/j.quageo.2015.02.015.

Ding, Z.L., Derbyshire, E., Yang, S.L., Yu, Z.W., Xiong, S.F., and Liu, T.S., 2002, Stacked 2.6-Ma grain size record from the Chinese loess based on five sections and correlation with the deep-sea δ18O record: Paleoceanography, v. 17, https://doi.org/10.1029/2001PA000725.

Fu, J., 2009, The fluvio-lacustrine landform development and environmental change in the Sanmenxia section of the Yellow River: Peking University, 1–115 p. [in Chinese with English abstract]

Fu, J., Zhang, K., Ma, Z., Wang, S., and Wu, Y., 2013, The terrace(T5 and T4)formation since the late Middle Pleistocene and its implication in the through cutting of the middle reach of Yellow River: Earth Science Frontiers, v. 20, p. 166–181 [in Chinese with English abstract].

Galbraith, R.F., Roberts, R.G., Laslett, G.M., Yoshida, H., and Olley, J.M., 1999, Optical dating of single and multiple grains of quartz from jinmium rock shelter, northern australia: part i, experimental design and statistical models*: Archaeometry, v. 41, p. 339–364, https://doi.org/10.1111/j.1475-4754.1999.tb00987.x.

Li, X., Liang, H., Zhang, K., Li, Z., Gong, W., and Fu, J., 2020, Depositional Characteristics of the Houma-Yuncheng Basin and Its Response to Tectonic Activity, Climate Change, and River Evolution: Chenji Xuebao, v. 38, p. 306–318 [in Chinese with English abstract].

Meng, Y.M., Zhang, J.F., Qiu, W.L., Fu, X., Guo, Y.J., and Zhou, L.P., 2015, Optical dating of the Yellow River terraces in the Mengjin area (China): First results: Quaternary Geochronology, v. 30, p. 219–225, https://doi.org/10.1016/j.quageo.2015.03.006.

Murray, A.S., and Wintle, A.G., 2000, Luminescence dating of quartz using an improved single-aliquot regenerative-dose protocol: Radiation Measurements, v. 32, p. 57–73, https://doi.org/10.1016/S1350-4487(99)00253-X.

Prescott, J.R., and Hutton, J.T., 1994, Cosmic ray contributions to dose rates for luminescence and ESR dating: Large depths and long-term time variations: Radiation Measurements, v. 23, p. 497–500, https://doi.org/10.1016/1350-4487(94)90086-8.

Wang, S., Jiang, F., Fu, J., Li, C., Cai, Y., Yao, H., Qiao, Y., Zhang, Z., and Li, Y., 2013, Some knowledge of the formation of the Yellow River: Quaternary Research, v. 33, p. 705–714 [in Chinese with English abstract].